ASME Journal of Biomechanical Engineering
Online journal at:
https://asmedigitalcollection.asme.org/biomechanical

Optimization of Active Backpack Loading Patterns to Improve the Walking Performance for Individuals With a Unilateral Transtibial Amputation

Mila M. Wetz
Walker Department of Mechanical Engineering,
The University of Texas at Austin,
204 East Dean Keeton Street,
Austin, TX 78712-1591
e-mail: milawetz@utexas.edu

Glenn K. Klute
Department of Veterans Affairs,
Puget Sound Health Care System,
1660 South Columbian Way, MS-151,
Seattle, WA 98118;
Department of Mechanical Engineering,
University of Washington,
3900 East Stevens Way NE,
Seattle, WA 98195
e-mail: gklute@uw.edu

Richard R. Neptune[1]
Walker Department of Mechanical Engineering,
The University of Texas at Austin,
204 East Dean Keeton Street,
Austin, TX 78712-1591
e-mail: rneptune@mail.utexas.edu

Individuals with unilateral transtibial amputation (TTA) often demonstrate asymmetrical gait patterns, which are further exacerbated during load carriage as passive prostheses cannot modulate their mechanical stiffness to accommodate the increased demand. Load carriage also increases the loads on the intact limb that can lead to overuse injuries and is also associated with increased metabolic cost and decreased forward propulsion. While active and passive load-suspended backpacks have been studied in healthy populations, no studies have explored the use of active backpacks to improve the walking performance for individuals with TTA. Therefore, the purpose of this study was to identify active backpack loading patterns to improve the metabolic cost, forward propulsion, and knee joint loading of individuals with TTA using a musculoskeletal simulation-based optimization framework. Different loading patterns were simulated using a time-varying actuator force applied to an active backpack over the gait cycle. The magnitude and timing of the actuator force were optimized for each performance criterion that resulted in a unique actuation pattern for each biomechanical measure. Interestingly, similar improvements relative to a passive backpack were observed across all actuation patterns, regardless of the optimization criteria. With all active backpacks, the force impulse experienced by the body from the dynamic load decreased, which resulted in increased forward propulsion, decreased intact knee joint loading, and improved metabolic cost. This suggests that active backpacks have the potential to improve walking performance during load carriage for individuals with TTA.
[DOI: 10.1115/1.4071641]

Keywords: musculoskeletal modeling, simulation, gait, biomechanics, performance measures

1 Introduction

Individuals with unilateral transtibial amputation (TTA) often exhibit asymmetrical gait patterns and biomechanical compensations due to the loss of important muscles crossing the ankle joint [1], which play a crucial role in essential functions such as body support, forward propulsion, and balance control [2–4]. Typically, passive prostheses attempt to replicate the function of the ankle muscles through the storage and release of elastic energy during the stance phase (e.g., Ref. [5]). However, without active ankle muscle force generation, individuals with TTA must utilize compensatory mechanisms that can adversely affect the intact limb. Individuals with TTA exhibit a shorter stance phase and longer swing phase on the residual limb, and therefore longer stance times on the intact limb [6] that increases the load on the intact side. This asymmetry imposes increased hip and knee moments and higher peak ground reaction forces (GRF) on the intact limb during unloaded walking [7,8]. This reflects an overall redistribution of mechanical work toward the intact side. Consequently, this increased loading is associated with a higher prevalence of overuse injuries such as osteoarthritis in the intact knee [9]. Musculoskeletal modeling studies have further shown that peak axial contact forces at the intact knee that are associated with the development of osteoarthritis are greater in individuals with TTA than in nonamputees, with the vasti, hamstrings, and gastrocnemius among the primary contributors to these elevated joint contact forces [10].

These adverse compensatory mechanisms may further increase in response to load carriage [11]. Individuals with TTA lack residual limb ankle plantarflexors, and therefore rely more heavily on the intact limb to meet the increased mechanical demands imposed by carrying an external load [12]. Individuals using passive prosthetic feet experience suboptimal stiffness under altered load conditions, as the stiffness of the prosthetic foot remains fixed and cannot adapt to accommodate load variations or changing task demands throughout the gait cycle [13]. Carrying loads in the form of a backpack is very common in daily life, which creates an additional dynamic load that can significantly impact amputee walking

[1]Corresponding author.
Manuscript received November 21, 2025; final manuscript received April 7, 2026; published online May 5, 2026. Assoc. Editor: Trisha Kesar.

performance. During backpack load carriage, individuals with TTA exhibit increased knee flexion during weight acceptance on the intact limb, supported by increased eccentric knee power, and increased hip flexion on both limbs [11], with the intact limb bearing a disproportionate share of the additional load. Furthermore, load carriage increases the metabolic cost of walking [12] and amplifies the risk of intact limb knee osteoarthritis in TTA by increasing intact limb knee joint impulse as a compensatory strategy [14].

More recently, studies have assessed how active backpacks can influence the biomechanics and energetics of walking. Active, load-suspended backpacks can help reduce the amplitude of the dynamic load exerted on the body with assistance from spring and damping mechanisms and/or motors. Previous research has shown active backpacks can improve walking economy by reducing metabolic cost by ~8% in healthy populations [15]. By adjusting the timing of the assistance periods over the gait cycle, different biomechanical and energetic benefits can occur. For example, a previous study found that assistance during the double support phase can aid with ankle push-off and reduce the peak ankle plantarflexor moment [16]. They also found that reducing the downward force while the body center-of-mass (CoM) is rising can assist with knee extension and reduce the knee extensor moment [16]. However, no studies have examined whether active backpacks can provide similar benefits for individuals with TTA. It is important to consider that the biomechanical task demands of active backpack assistance differ fundamentally for individuals with TTA compared to able-bodied populations. In healthy gait, active unloading can be distributed symmetrically across both limbs, with the ankle plantarflexors playing a central role in absorbing and redistributing the dynamic load. In individuals with TTA, the absence of residual limb ankle plantarflexors shifts this burden asymmetrically to the intact side [14], suggesting that the primary target of active assistance may be the improvement of residual limb propulsion or the mitigation of intact limb overloading. Because intact limb overloading in TTA particularly occurs during weight acceptance and push-off [11], the timing of active backpack assistance must be tailored to these asymmetric demands rather than simply mirroring strategies developed for symmetric gait. In addition, the fixed stiffness of passive prosthetic feet cannot adapt to the fluctuating load demands experienced across the gait cycle [13], suggesting that conventional unloading strategies optimized for able-bodied users may be misaligned with the needs of users with a prosthesis.

Human subject studies have had success with improving biomechanical outcomes with an active backpack in healthy populations, but these iterative studies can be time consuming and demanding, especially for those with TTA. In contrast, musculoskeletal modeling and predictive simulation provide an efficient framework to investigate the effects of various active loading patterns on gait performance. Previous simulation studies of passive load carriage identified how different load carriage positions impact muscle function and propulsion, as well as joint loading [12,13]. However, no studies have assessed how different active backpack loading patterns influence the walking performance of individuals with TTA.

Therefore, the purpose of this study was to assess whether there are optimal active backpack loading patterns that improve the metabolic cost, forward propulsion, and knee joint load symmetry for individuals with TTA using a musculoskeletal simulation-based optimization framework. We expected to find distinct active backpack loading patterns that improve the metabolic cost, forward propulsion, and knee joint load symmetry relative to a traditional passive backpack. By elucidating the influence of dynamic loading patterns on biomechanical measures of TTA walking, this study will provide a framework for future studies seeking to improve other aspects of TTA walking performance.

2 Methods

2.1 Experimental Data. Lower limb kinematic and kinetic data were previously collected from five individuals with unilateral TTA (for a detailed description of the methods and protocol, see Ref. [17]). Lower-limb joint kinematics were recorded from reflective markers using a motion capture system (Vicon, Oxford, UK). Three-dimensional GRFs were also recorded as subjects walked at their self-selected speed over five overground force plates (AMTI, Watertown, MA) and normalized by body weight. The data were averaged across all trials and normalized to a single stride starting from the residual limb heel strike. Simulations were then generated to emulate the group averaged data from all subjects.

2.2 Musculoskeletal Model. A 2D musculoskeletal model (mass: 72.2 kg; height: 1.70 m) with ten degrees-of-freedom and 26 Millard-type musculotendon actuators (Supplemental Table 1 available in the Supplemental Materials on the ASME Digital Collection) was developed by augmenting the LaPrè model [18] with additional back and abdominal muscles. A passive prosthetic ankle was simulated using a coordinate actuator at the ankle joint to apply a proportional torque to achieve the desired experimentally measured ankle kinematics [13]. To model the foot–ground contact, two compliant Hunt–Crossley contact spheres were applied at the toe and heel of each foot [19]. The spheres had constant stiffness, damping, static friction, dynamic friction, and viscous friction coefficients of 2 MPa, 1 s/m, 0.9, 0.6, and 0.6, respectively [18].

To model the active backpack system that encompasses the pack's active elements and additional payload, a rigid-body that was 20% of the model's body weight (14 kg) with inertial properties adapted from Dembia et al. [20] was added to the trunk segment. The interface between the backpack and trunk was modeled using a slider joint with linear spring ($k = 45$ N/m) and damper ($b = 80$ N/(m/s)) coefficients that allowed for an oscillation range of ~5 cm.

2.3 Baseline Simulation Without a Backpack. The experimental data used for tracking was collected from TTA subjects without a backpack; therefore, an initial baseline simulation that emulated this data was generated without a backpack. The parameters from this simulation were then used as initial conditions for the optimizations with a backpack. One full gait cycle (GC) from one residual limb heel strike to the next was simulated using the predictive simulation and dynamic optimization software SCONE (v2.3.0) [21]. Initial muscle excitation patterns were shaped by four optimizable parameters (i.e., the start time, rise time, fall time, and peak amplitude) using the "Raise–Fall" profile functions native to SCONE. The optimizer stochastically selected values for the peak amplitude of the excitations from 0 to 1 (maximum stimulation), and the timing parameters were selected based on electromyographic timing from the literature [22,23] within ±10% of the gait cycle. The excitations were further refined using a reflexive feedback controller to stabilize the model based on the specific stage of the gait cycle and the dynamic interaction between the foot contact spheres and the ground [24]. The timing and magnitude of the excitations were optimized by minimizing a cost function using the covariance matrix adaptation evolution strategy [25]. For the unloaded TTA simulations, the cost function (J) (Eq. (1)) consisted of a weighted sum that penalized deviations of the predicted joint angles, horizontal position and velocity of the pelvis CoM, as well as vertical and anterior–posterior (AP) GRFs ($\hat{Y}_{ij}$) from the corresponding experimentally measured values (Y_{ij}). The error was normalized by the experimental variability of that variable (σ_j). This resulted in a total of $m = 12$ variables in the cost function (Eq. (1)). Equal weights ($w_j = 10$) were initially assigned to each variable, then based on the resulting error from each simulation, the weight of the variable with the greatest deviation from the experimental data was increased in increments from 1 to 5. Multiple optimizations were run in sequence, and the results from the simulation with the lowest cost function value were used to initialize the next optimization. The weights were adjusted, and the process was repeated until the unloaded TTA baseline simulation tracked the experimental data within ±2 standard deviations to establish a reference for the subsequent loaded simulations.

$$J = \sum_{j=1}^{m} w_j \sum_{i=1}^{n} \frac{\left(Y_{ij} - \hat{Y}_{ij}\right)^2}{\sigma_j} \quad (1)$$

2.4 Simulations With an Active and Passive Backpack. After this baseline simulation successfully replicated the experimental data, a separate 14 kg mass was added to the trunk segment to represent the backpack system with a payload. The passive backpack's range of motion was constrained to 5 cm, with coordinate limit forces applied at the top and bottom of the slider joint between the backpack and trunk. This allowed for limited relative motion between the trunk and backpack. Another term was incorporated into the cost function to penalize excessive pelvic tilt and assure postural stability under the additional load. The optimization process was repeated, and the cost function weights were adjusted to allow for expected kinematic deviations due to the added load. Next, the active backpack condition followed the same simulation framework as the baseline simulation but included a linear coordinate actuator acting on the backpack. Different loading patterns were simulated by applying varying magnitudes of force to the backpack using this actuator (i.e., actuation pattern). These actuation patterns were determined by a parameterized curve, which defined the magnitude and timing of the actuation pattern. These parameters were optimized based on additional walking performance criteria (Eq. (2)). The resulting impulse produced by the backpack with these actuation patterns was calculated as the time integral of the total force transmitted to the body, including both passive forces from the backpack joint's spring and damping elements and the active force from the actuator.

2.5 Walking Performance Criteria. To increase residual limb propulsion (PROP), a propulsion measure (J_{Prop}) and associated weighting factor ($w_{\text{Prop}} = 5$) were added to the cost function (Eq. (2)). This term was calculated by integrating the positive portion of the normalized AP GRF curve during the residual limb push-off phase (30–60% GC) (Fig. 1(*b*)). The simulated GRFs were normalized by total weight, which included both the body weight and additional pack weight. Simulations with higher J_{Prop} values were favored and the weight of each term was adjusted to produce the lowest cost function value while maintaining kinematics and GRFs that mimicked experimental values within ±2 standard deviations. To minimize metabolic cost (EFFORT), the propulsion measure was replaced with an effort measure (J_{Effort}) and weighting factor ($w_{\text{Effort}} = 0.0001$) that minimized metabolic cost of transport over one gait cycle while maintaining consistent walking speed, kinematics and GRFs. This measure was computed using the Bhargava metabolic cost model [26], and the cost function weights were readjusted accordingly. Finally, to reduce the intact knee joint loads, a knee joint contact force (KJCF) measure (J_{KJCF}) was introduced to minimize the axial intact knee joint contact force. This measure penalized simulations exhibiting high joint contact forces, and the cost function was readjusted with a new weighting factor ($w_{\text{KJCF}} = 5$). The axial tibiofemoral joint contact force was obtained in both the intact and residual limbs and the time integral was computed over their respective stance phase to determine the joint contact impulse for each simulation [12]. In addition, peak sagittal plane knee extensor and flexor moments were determined for each simulation and normalized by total body weight.

$$J = \sum_{j=1}^{m} w_j \sum_{i=1}^{n} \frac{\left(Y_{ij} - \hat{Y}_{ij}\right)^2}{\sigma_j} + w_{\substack{\text{Performance} \\ \text{Measure}}} * J_{\substack{\text{Performance} \\ \text{Measure}}} \quad (2)$$

2.6 Mechanical and Muscle Work Analysis. To help interpret the influence of the active backpacks on muscle demand, a post-hoc analysis of muscle work was performed using OPENSIM 4.5 [27]. Muscle power from each simulation was integrated over each phase of the gait cycle to compute muscle work for all muscles individually. To aid interpretation, the muscles were combined into functional groups [28] (Supplemental Table 1 available in the Supplemental Materials on the ASME Digital Collection). The work done by each functional group and a selection of key individual muscles were analyzed. Positive (negative) work was defined as concentric (eccentric) work.

To assess the impact of the optimized actuation patterns on the prosthesis energy storage and return, the residual limb ankle power was calculated by multiplying the moment at the prosthesis ankle joint by its corresponding angular velocity. Positive (negative) power delivered by the prosthesis indicated that the moment was applied in the same (opposite) direction as the velocity. Each stance phase was subdivided into two regions: loading (0–30% GC) and push-off (30–60% GC) (Fig. 1(*b*)). The prosthesis power was integrated over both regions of the stance phase to determine the work done during loading and push-off. The energy return ratio of the prosthesis was defined as the positive work divided by the magnitude of negative work, representing the proportion of stored energy that was returned.

3 Results

3.1 Optimized Backpack Actuation Patterns. When optimizing for different performance criteria, the resulting backpack actuation patterns (Fig. 1(*a*)) produced varying impulses at different phases of the gait cycle (Fig. 1(*b*)). Overall, the downward impulse applied to the body by the backpack was significantly reduced throughout the entire GC in all simulations with an active backpack relative to the passive backpack. Furthermore, in specific regions of the GC, the optimized backpack actuations applied a small upward impulse. The PROP and KJCF actuations provided an upward impulse during residual limb early stance. During residual limb midstance, the PROP, KJCF, and EFFORT actuations provided a downward impulse. During residual limb late stance, all actuations provided an upward impulse. In residual limb early swing, all actuations provided a downward impulse. Finally, in residual limb late swing, the EFFORT and PROP actuations provided an upward impulse.

3.2 Simulated Joint Angles and GRFs. Overall, the simulations emulated well the experimental data (Figs. 2(*a*) and 2(*b*)). In simulations with a passive backpack (PASS), the predicted sagittal plane joint angles for the hip and ankle were within 2 standard deviations (SD) of experimental unloaded data (Fig. 2(*a*)). However, the intact knee demonstrated less extension (−2.8 SD), and the residual knee demonstrated more extension (+2.8 SD) compared to the unloaded experimental average (Fig. 2(*a*)). The predicted intact knee and ankle angles with all three active backpacks mimicked the unloaded, experimental joint angles more closely than with the passive backpack (Fig. 2(*a*)). Likewise, the predicted, normalized intact limb GRFs in both the vertical and AP directions were within 2 SD of the experimental unloaded TTA walking data (Fig. 2(*b*)).

The PROP simulation demonstrated a larger positive AP GRF duration in the residual limb compared to the passive condition (Fig. 2(*b*)) and a reduction in the second peak of the residual limb vertical GRF curve. In addition, the positive residual limb AP GRF peak was delayed from the PASS simulation (+7% GC), while for both the KJCF and EFFORT simulations the positive AP GRF peak occurred slightly earlier (−3% GC) compared to the PASS simulation (Fig. 2(*b*)). The residual limb AP GRF impulse during push-off (30–60% GC) increased by 31%, 22%, and 18% for the PROP, KJCF, and EFFORT simulations, respectively, compared to the PASS simulation (Fig. 2(*c*)).

3.3 Metabolic Cost of Transport. The metabolic cost of transport for the residual limb stance phase (0–60% GC) decreased

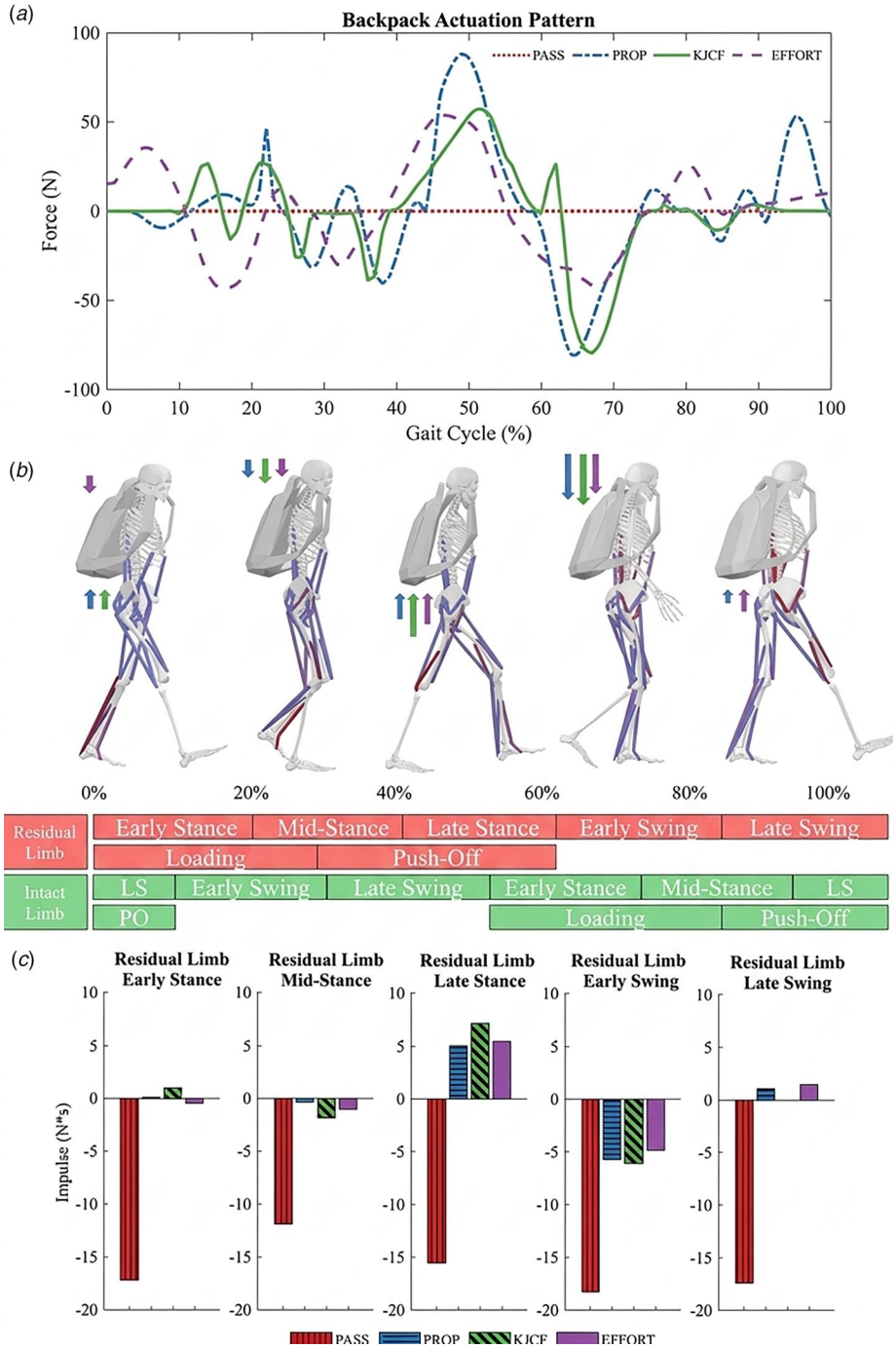

Fig. 1 (*a*) **The optimized actuation patterns applied to the backpack in the PROP (dotted hash), KJCF (solid), EFFORT (dashed), and PASS (dotted) simulations. Positive (negative) force indicates force applied upward (downward) on the backpack CoM. (*b*) The model's position in each region of the gait cycle: early stance (residual: 0–20% GC; intact: 50–70% GC), midstance (residual: 20–40% GC; intact: 70–90% GC), late stance (LS) (residual: 40–60% GC; intact: 90–100% and 0–10% GC), early swing (residual: 60–80% GC; intact: 10–30% GC), and late swing (residual: 80–100% GC; intact: 30–50% GC). Each stance phase was further subdivided into a loading phase (residual: 0–30% GC; intact: 50–80% GC) and a push-off (PO) phase (residual: 30–60% GC; intact: 80–100% and 0–10% GC). The arrows indicate the relative impulse experienced by the body from the dynamic load during the PROP (dash-dot), KJCF (solid), and EFFORT (dashed) simulations. (*c*) Impulse from the backpack applied to the body across the different regions of the gait cycle, resulting from the passive force from the backpack joint's spring and damping elements and the active force from the actuator for the PASS (vertical striped), PROP (horizontal striped), KJCF (diagonal striped), and EFFORT (solid) simulations.**

for both the PROP and EFFORT simulations by 7% and 8%, respectively, but increased for the KJCF simulation by 9% relative to the PASS simulation (Fig. 3(*a*)). The metabolic cost of transport during intact limb stance (0–10% GC and 50–100% GC) decreased for both the KJCF and EFFORT simulations by 10% and 16%, respectively, but increased for the PROP simulation by 19% relative to the PASS simulation (Fig. 3(*b*)). Overall, the total metabolic cost for the full gait cycle decreased in the KJCF and EFFORT simulations by 6% and 12%, respectively, and increased in the PROP simulation by 5% relative to the PASS simulation (Fig. 3(*c*)).

3.4 Knee Joint Loading and Moments. The total axial knee joint contact force in the intact limb decreased in all active backpack simulations compared to the PASS simulation (Fig. 4). The axial intact knee joint contact impulse decreased by 4%, 21%, and 12%, in the PROP, KJCF, and EFFORT simulations, respectively, relative to the PASS simulation (Fig. 4). The symmetry of the impulse experienced by both joints improved in the KJCF simulation. During intact limb early stance, the peak knee extensor moment decreased in both the KJCF and EFFORT simulations compared to the PASS simulation, while the peak knee flexor moment remained consistent during midstance with the PASS simulation (Supplemental Table 2 available in the Supplemental Materials on the ASME Digital Collection).

3.5 Prosthesis Mechanical Work. Changes in the magnitude of the energy stored and returned by the prosthesis during the residual limb loading and push-off regions were observed in all three simulations (Fig. 5). In the PROP, KJCF, and EFFORT simulations, roughly twice the amount of negative work was performed by the prosthesis during loading compared to the PASS simulation (Fig. 5). This resulted in a proportional increase in the amount of positive

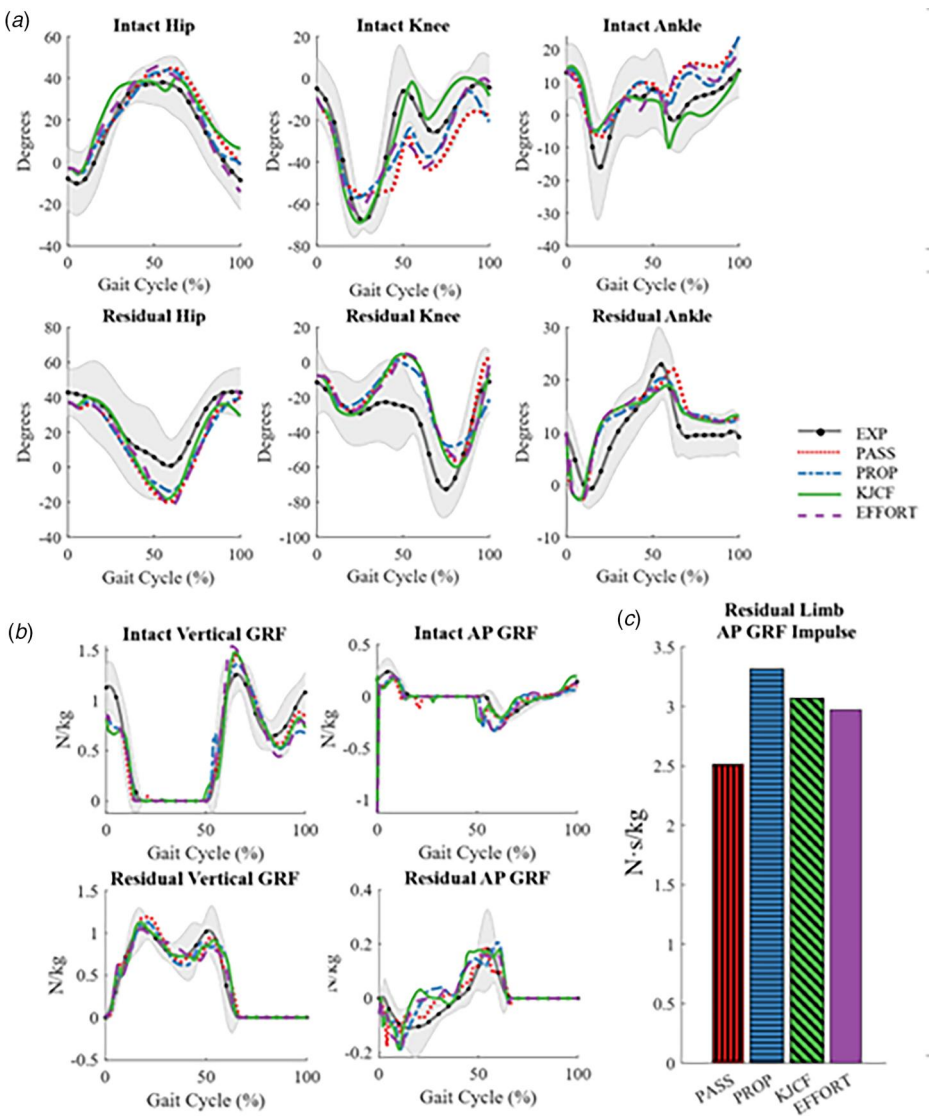

Fig. 2 (*a*) Joint angles and (*b*) GRFs for the intact (top row) and residual (bottom row) limb from simulations optimized for propulsion (dotted hash), KJCF (solid), and metabolic cost (dashed) compared to the joint angles and GRFs from simulations with a passive backpack (dotted). The 0% GC corresponds with residual limb heel contact. Initial intact limb heel contact occurs at 50% GC. Experimental, unloaded TTA joint angle and GRF data (grey and black ticked) ±2 standard deviations (shaded region) are shown for reference. (*c*) The magnitude of the residual limb push-off phase AP GRF impulse increased from the PASS (vertical striped) in the PROP (horizontal striped), EFFORT (diagonal striped), and KJCF (solid) simulations. As each condition represents a single predictive simulation, error bars are not displayed.

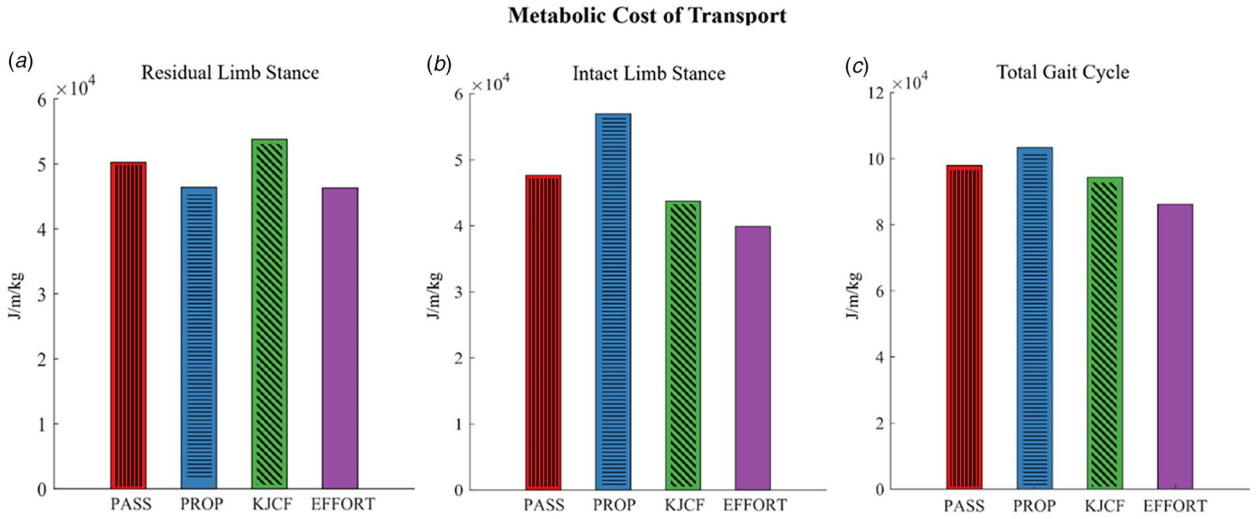

Fig. 3 The metabolic cost of transport for (*a*) residual limb stance (0–60% GC), (*b*) intact limb stance (0–10% and 50–100% GC), and (*c*) total gait cycle for the PASS (vertical striped), PROP (horizontal striped), KJCF (diagonal striped), and EFFORT (solid) simulations. As each condition represents a single predictive simulation, error bars are not displayed.

work delivered during push-off. The overall energy return ratio remained similar for all simulations with a slight increase in energy return in the PROP and EFFORT simulations (Fig. 5).

3.6 Muscle Work. The magnitude of positive work performed by the residual hip extensors in early stance decreased with all actuation patterns (Fig. 6 right column). During residual limb early and midstance, there was a decrease in residual Vasti (VAS) work in all simulations with an active backpack (Fig. 7 right column). During residual limb midstance, flexor work decreased in all simulations with an active backpack (Fig. 6 right column). The reduction in flexor work was primarily due to a decrease in residual limb iliopsoas (IL) work in this phase (Fig. 7 right column). During intact limb loading in the PROP simulation, the negative work performed by the knee extensors increased. In early and midstance, the magnitude of work required by the intact knee extensors decreased in all simulations (Fig. 6 left column). This was driven primarily by a decrease in the intact limb VAS work during early stance (Fig. 7 left column). In early stance, an increase in intact hip extensor work was observed with the PROP and KJCF actuation patterns (Fig. 6 left column).

4 Discussion

The objective of this study was to assess whether there are optimal active backpack loading patterns that improve various aspects of walking performance for individuals with TTA using a musculoskeletal simulation-based optimization framework. We expected to identify distinct backpack loading patterns that would improve the metabolic cost, forward propulsion, and knee joint loading relative to a traditional passive backpack. This was partially supported as, overall, distinct backpack loading patterns were observed when optimizing for the different outcome measures. However, similar improvements were observed with all active backpack loading

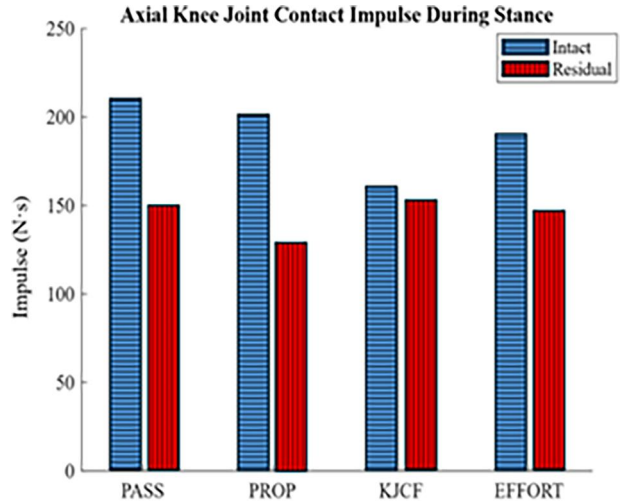

Fig. 4 The axial knee joint contact impulse in both the intact (horizontal striped) and residual (vertical striped) limbs in the PROP, KJCF, and EFFORT simulations compared to the PASS simulation. As each condition represents a single predictive simulation, error bars are not displayed.

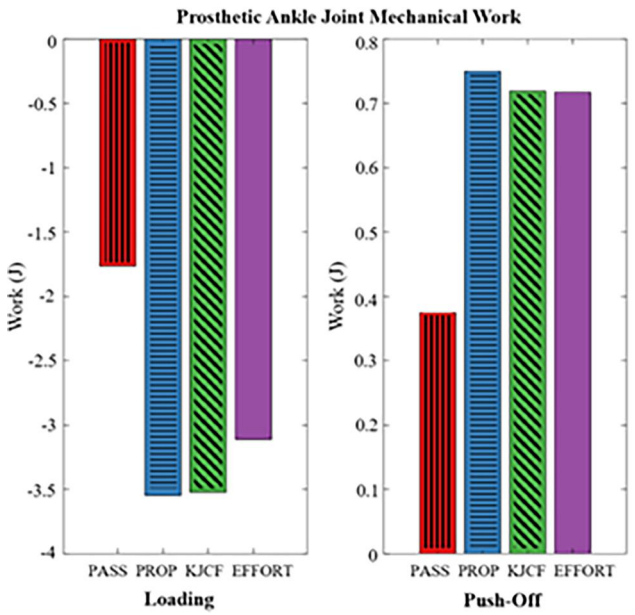

Fig. 5 The magnitude of mechanical work performed by the prosthesis during loading (0–30% GC) and push-off (30–60% GC) in the PROP (horizontal striped), KJCF (diagonal striped), EFFORT (solid), and PASS (vertical striped) simulations. As each condition represents a single predictive simulation, error bars are not displayed.

patterns relative to a passive backpack. For example, regardless of associated cost function terms, all simulations with an active backpack demonstrated increased forward propulsion and prosthesis mechanical work, which resulted in decreased intact knee loading and helped restore a normal gait pattern. This suggests that, overall, walking with an active backpack is more beneficial than walking with a passive one for individuals with TTA.

4.1 Kinematic and Kinetic Changes With an Active Backpack. Across all active backpack simulations, joint kinematics more closely resembled the unloaded TTA gait patterns than those observed in the PASS simulation, with the greatest improvements occurring in the intact limb. All active backpack simulations resulted in more intact knee extension during intact limb loading compared to the PASS simulation, which may be beneficial as individuals with TTA often exhibit increased intact knee flexion during stance when carrying a load [11]. Similar reductions in knee flexion during early stance have also been reported in active backpack studies aiming to reduce metabolic cost in healthy individuals [29]. Typical adaptations in loaded TTA gait also include altered intact ankle plantarflexion during weight acceptance and push-off [11]. For all simulations with an active backpack, the intact ankle angle during stance aligned more closely with the unloaded gait pattern, which suggests improved ankle motion with assistance from the active backpack.

In the residual limb, the prosthetic ankle demonstrated increased dorsiflexion during early stance, indicating greater energy storage by the prosthesis [30] in all active backpack simulations. During midstance, the prosthesis entered plantarflexion earlier as this stored energy was subsequently released throughout midstance and was associated with increased mechanical work performed by the ankle and an increase in the peak positive AP GRF in the PROP simulation relative to the PASS simulation. In all active backpack simulations, the onset of positive AP GRF in the residual limb occurred earlier in the gait cycle compared to the PASS simulation. This extended the duration of propulsion, resulting in a larger positive AP GRF impulse relative to the PASS simulation. These findings are consistent with previous work that has explored the relationship between prosthesis energy return and propulsive GRF impulses [5,30].

The residual limb AP GRF impulse for the KJCF and EFFORT actuation pattern increased, despite the absence of a propulsion-specific term in the cost function. This enhancement in residual limb propulsion likely contributed to improved interlimb symmetry, which has been associated with reduced joint contact forces in individuals with TTA [31]. By redistributing the mechanical workload, the KJCF actuation pattern helped alleviate excessive loading on the intact knee joint. This is consistent with previous studies that have shown devices enhancing propulsion on the prosthesis side can help to alleviate loading on the intact limb [32] and decrease metabolic cost [33].

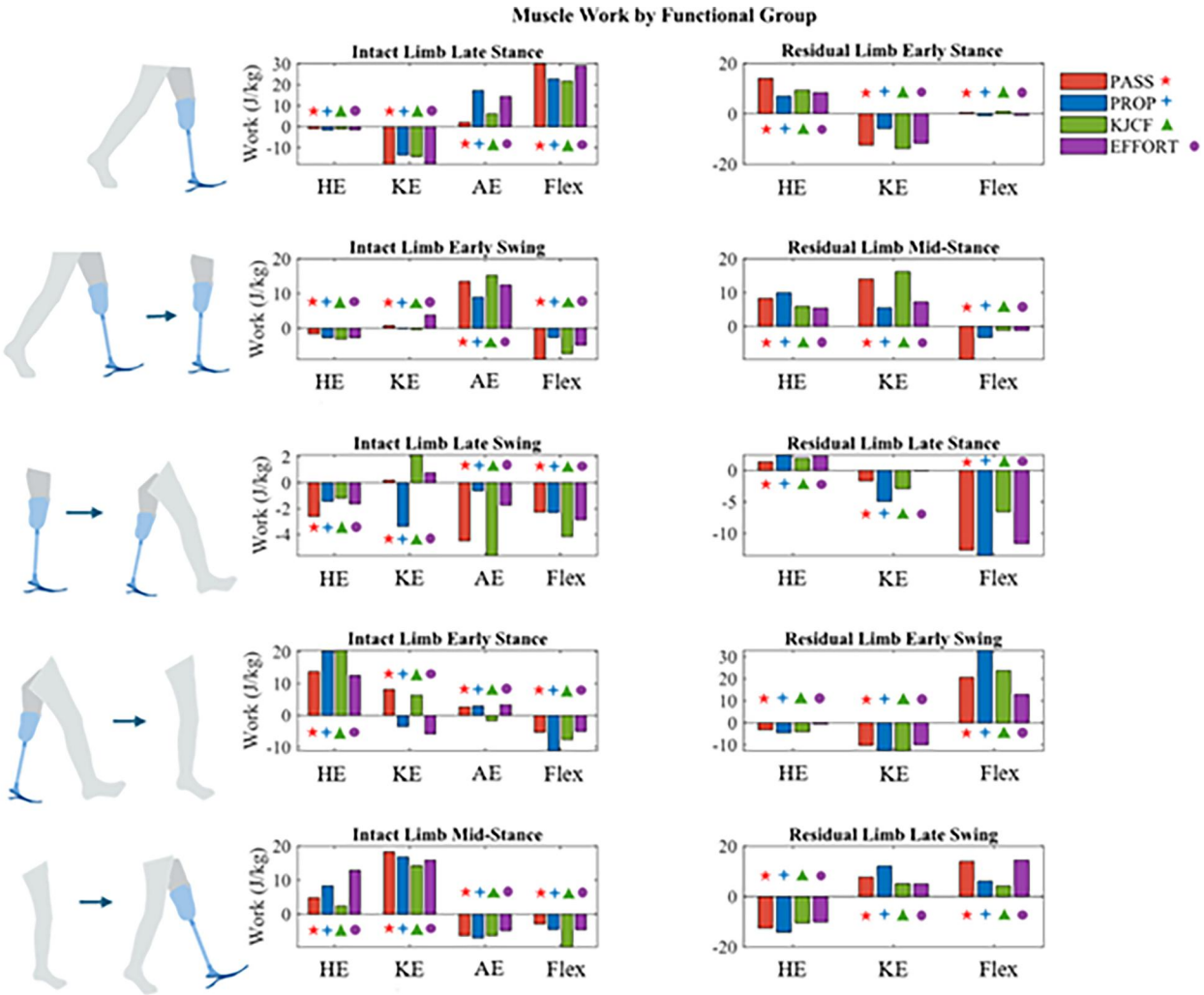

Fig. 6 The work performed in each region of the gait cycle by each of the muscle groups: hip extensors (HE), knee extensors (KE), and flexors (Flex) in both the intact (left column) and the residual (right column). The results from the different simulations, PASS (star), PROP (plus), KJCF (triangle), and EFFORT (circle), are distinguished using colors and symbols to assist with identification when color resolution is limited.

4.2 Metabolic Cost Reduction With an Active Backpack. The actuation pattern optimized to reduce metabolic cost achieved lowered costs of transport by decreasing the dynamic load impulse experienced by the body. The results from all active backpack simulations align with other studies that have successfully reduced the metabolic cost of load carriage by reducing the impulses experienced by the body from a passive load [29,34]. During midstance, when the CoM rises, all active backpacks reduced the downward impulse experienced by the body, suggesting that these actuation patterns helped to decrease the demand for body support during the phase of the gait cycle when it is metabolically expensive [28]. Similar reductions in metabolic cost have been observed in previous experimental active backpack studies [16]. In addition, the backpack actuator provided an upward impulse during the double support phase in all active backpack simulations. By providing assistance during double support, when energy is being used to redirect the body CoM, the active backpacks help reduce the metabolic cost during a gait phase that is energetically demanding [28].

4.3 Muscle Work Analysis With an Active Backpack. The muscle work analysis determined that the magnitude of positive work performed by the residual hip extensors in early stance decreased with all actuation patterns (Fig. 6 right column). Previous research has highlighted that individuals with TTA demonstrate increased residual limb hip extensor work in early stance when the task demands increase by walking at increasing speeds [35]. The decrease in positive hip extensor work suggests that these actuation patterns may assist with alleviating the demand for these muscles during load carriage. These muscles are primarily involved in body support during this phase of the gait cycle [36], which supports the observation that the active backpacks assist with decreasing the demand for body support. During residual limb midstance, flexor work decreased in all simulations with an active backpack (Fig. 6 right column). The reduction in flexor work was primarily due to a decrease in residual limb IL work in this phase (Fig. 7 right column). Typically, during load carriage, the work required by the residual hip flexors during stance increases as individuals with TTA rely on the hip to adapt to added load [11,37]. Thus, the reduction in hip flexor work with an active backpack suggests a reduced need for compensation at the residual limb hip joint.

During intact limb loading in the PROP simulation, the negative work performed by the knee extensors increased. When optimizing solely for propulsion, the increased work generated by the residual limb required greater energy absorption in the intact limb during loading. This helps explain the observed increase in metabolic cost during intact limb stance in the PROP simulation. Typically, in early and midstance, there is an increase in intact knee extensor power generation when an external load is present [11]. However, in early and midstance, the magnitude of work required by the intact knee extensors decreased in all simulations. In early stance, an increase in intact hip extensor work was observed with the PROP and KJCF actuation patterns. This suggests that these actuation patterns may result in a tradeoff between the intact hip and knee work required during stance. Similarly, other studies investigating active backpack

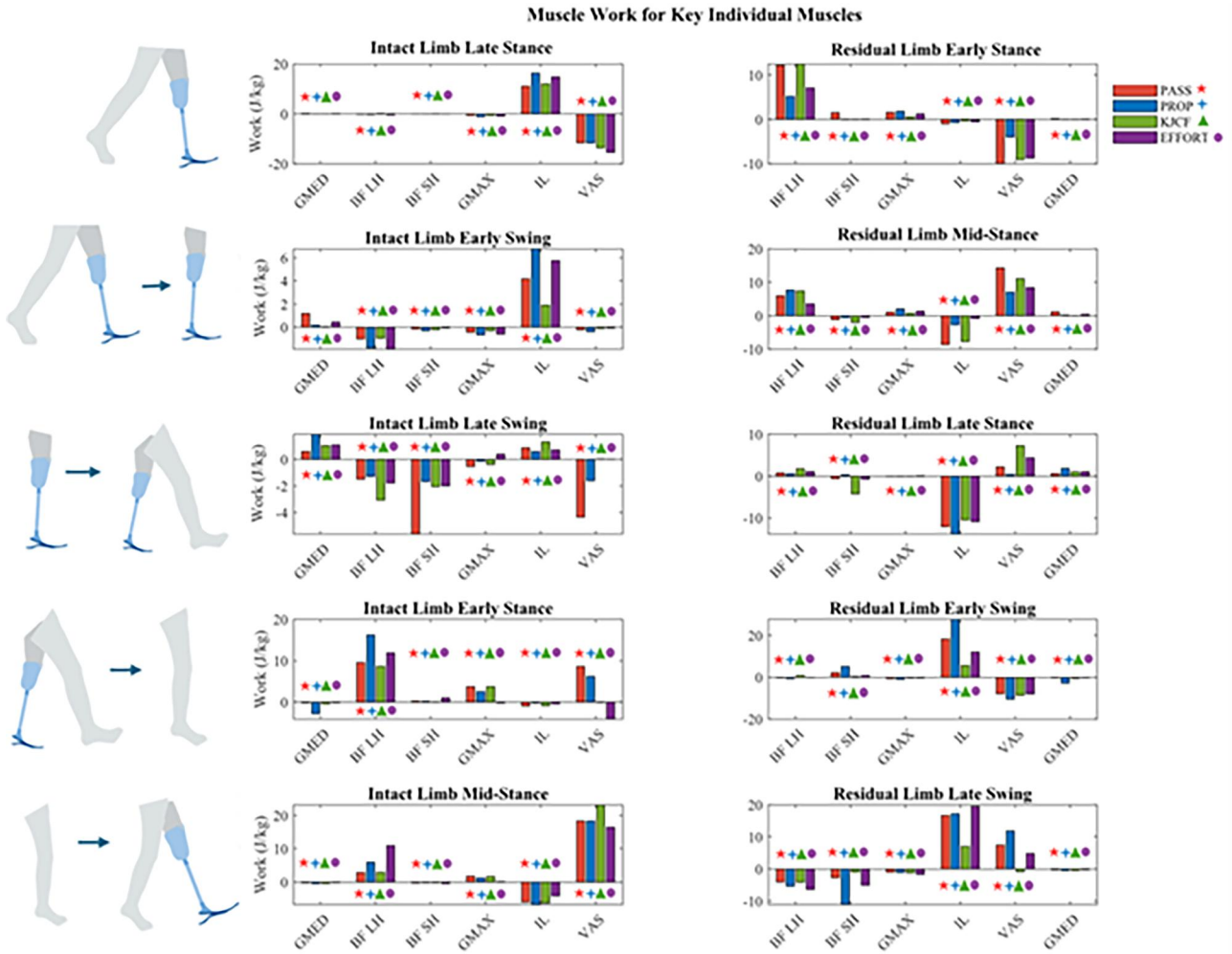

Fig. 7 The work performed in each region of the gait cycle by key muscles in both the intact (left column) and the residual (right column) limbs in the PASS (star), PROP (plus), KJCF (triangle), and EFFORT (circle) simulations

assistance in able-bodied individuals have reported reductions in knee extensor activity during midstance when seeking to minimize metabolic cost [29]. These findings suggest that knee extensor demands during midstance may represent a substantial portion of the metabolic burden during load carriage [38]. Thus, these actuation patterns may assist with reducing the metabolic demand of load carriage by redistributing some of the workload to the hip joint.

4.4 Joint Loading and Moment Improvements With an Active Backpack. The total axial knee joint contact impulse was reduced with all active backpack patterns, primarily by decreasing the load impulse experienced by the body from the backpack and increasing residual limb propulsion [39]. The KJCF actuation pattern reduced the magnitude of joint loading in both limbs by providing an upward force as the CoM descends, thus reducing the downward acceleration of the backpack during residual and intact loading phases. Previous studies have observed a 14–20% increase in intact knee joint contact impulse when individuals with TTA carry a back load that is 17% of their body weight [12]. This suggests that the 23% reduction observed with the KJCF actuation pattern (Fig. 5) could almost fully restore the intact knee joint contact impulse to those observed in unloaded TTA gait. The reduced impulse from the backpack during midstance also assisted with decreasing the knee extensor moment in the KJCF and EFFORT simulations (Supplemental Table 2 available in the Supplemental Materials on the ASME Digital Collection). This aligns with previous work demonstrating that decreasing the load force when the CoM is rising assists knee extension and reduces knee extensor moment in healthy populations [16].

In the active backpack simulations, there was also a decrease in the magnitude of muscle work performed by the intact VAS during early stance (Fig. 7 left column) and by the residual VAS during early and midstance (Fig. 7 right column). VAS is a major contributor to the axial knee joint contact force during unloaded walking [10], and VAS activity has been shown to increase as the demand for body support increases [40]. In addition, increased VAS contribution to body support has been associated with more asymmetric knee joint loading in individuals with TTA [41]. This suggests that by reducing the demand for body support, and thus lowering VAS work, these actuation patterns contributed to lower intact knee joint loading. If the reductions in knee joint contact impulse predicted here are experimentally confirmed, an active backpack system could meaningfully reduce the joint loading associated with load carriage, potentially enabling individuals with TTA and knee osteoarthritis to carry similar loads. This would represent a clinically meaningful advancement for this population, making load carriage more accessible and improving overall quality of life for individuals with TTA.

4.5 Limitations and Future Work. This study used musculoskeletal modeling and predictive simulations to investigate the effects of optimized active backpack actuation patterns on gait kinematics and kinetics, metabolic cost, and knee joint contact forces for individuals with TTA. When interpreting these results, a number of limitations should be considered. First, the experimental tracking data that were used to inform the motion of the simulations were collected from a sample of five individuals with TTA during unloaded walking. The small sample size of experimental tracking data limits the generalizability of the simulation results to the broader TTA population. It should be noted that each condition is represented by a single predictive simulation output. Therefore, traditional descriptive statistics and effect sizes cannot be calculated. The magnitude of observed effects is therefore conveyed through percentage differences between conditions. The percentage changes reported throughout the results reflect descriptive comparisons between conditions rather than formally defined thresholds for a statistically significant change. Similarly, the ±SD thresholds used to contextualize kinematic and kinetic deviations are derived from the experimental, unloaded gait data of a small sample of five participants and may not fully capture the natural variability in gait across the broader TTA population. The experimental data also does not account for predictable gait changes that occur during load carriage. To account for expected gait adaptations under the additional load, the weights of the tracking terms in the cost function were reduced in the load carriage simulations. Consequently, simulation outputs deviated from the original unloaded experimental kinematics by more than two standard deviations during different regions of the gait cycle. However, these deviations aligned with typical compensatory strategies observed in loaded TTA gait [11], suggesting that the simulations were able to capture realistic adaptations. In addition, the passive prosthetic ankle angles were simulated using a torque actuator and a proportional–derivative controller to replicate the experimental kinematics. Therefore, the prosthetic ankle in the simulations is not a purely passive joint; however, the resulting mechanical work output was comparable to that of other energy storing and releasing prosthesis models [5]. It should also be acknowledged that every simulation variable was optimized with each cost function, including muscle activations, such that this large number of simultaneously changing variables could influence the observed gait changes attributed to the optimization criteria. The resulting multiplicity of dependent variables and comparisons across conditions increases the risk that some observed differences may not reflect true biomechanical changes, but instead are artifacts of the optimization. However, this concern is partially mitigated by enforcing kinematic and kinetic tracking and holding the simulated distance and velocity constant for all simulations.

It is also important to consider that the simulations were performed with a 2D model, so changes in the frontal plane could not be observed. Importantly, several studies have associated the increased risk of osteoarthritis with greater knee adductor moments in the frontal plane (e.g., Ref. [42]). Therefore, future work should analyze the impact of active backpacks using a 3D musculoskeletal model to fully observe their influence on the knee joint contact force.

A final potential limitation of this work is the unlimited flexibility of the backpack actuator used in the simulations. The magnitude and timing of the forces applied by the actuator were unconstrained by potential hardware limitations. In contrast, a physical active backpack system would be limited by the mechanical design and motor capacity. However, the optimized actuation patterns did not demonstrate any large instantaneous changes in force or direction that would be unrealistic to produce with motors previously used in active backpacks [43]. Further, the active backpack system was modeled as a 14 kg load, which included the weight of active elements and an additional payload. Previous studies have reported the weight of active components to be around 5.3 kg (e.g., Refs. [15] and [29]) and have analyzed load suspended backpacks between 15 kg [29] and 27 kg [34]. The weight of active backpack systems should be optimized to ensure that the benefits of the active backpack are not offset by the metabolic burden of the hardware itself.

A natural extension of this work is the development of a physical active backpack system and corresponding controller capable of replicating the optimized loading patterns. This system would provide a valuable opportunity to experimentally validate the simulation results in the TTA population and would help establish the translational potential of this simulation framework. Importantly, experimental validation in the TTA population presents unique challenges, as there are a wide range of prosthesis types, residual limb lengths, and activity levels. These factors could influence how individuals respond to active backpack assistance. Recruiting a sample large enough to account for this variability while maintaining adequate statistical power would therefore be an important consideration in the design of future experimental studies. In addition, fatigue and evolving compensatory strategies over the course of a testing period may make it challenging to isolate the effects of the backpack actuation pattern itself. It is also important to consider the rapid changes in vertical acceleration produced by the active backpack actuator (Supplemental Fig. 1 available in the

Supplemental Materials on the ASME Digital Collection) may present additional challenges for the user. The dynamic shifts in load distribution could be uncomfortable or destabilizing for individuals with TTA, who already experience significant balance control deficits that can increase their risk of falls [44]. Notably, the results of the present study indicate that the loading pattern resulting from the EFFORT optimization produced favorable outcomes in all evaluated categories and may represent the most broadly beneficial loading pattern to improve overall gait in individuals with TTA. In addition, the exploration of a semipassive backpack system, in which springs and dampers are tuned to approximate the EFFORT actuation pattern, may provide a lightweight, simple solution resulting in similar overall benefits. This approach may produce smoother, more gradual load transitions that could be more easily adapted by individuals with TTA.

Future studies should also seek to improve other aspects of walking performance with active backpacks, such as balance control. While measures were incorporated into the cost function to penalize deviations in sagittal plane trunk angle and velocity, more targeted analyses could be performed to assess whether active backpacks can improve balance control during different walking conditions to decrease the risk of falling for individuals with TTA. Finally, although the weighting factors used in the optimization improved the various aspects of walking performance, future work should also explore how robust the results are to variations in those weighting factors.

5 Conclusion

In summary, we have shown using modeling and simulation that active backpacks can improve various biomechanical and energetic measures during load carriage for individuals with TTA. All active backpack actuation patterns assisted with decreasing the load impulse acting on the body compared to walking with a passive load. These improvements were associated with reduced metabolic cost, greater forward propulsion, and reduced intact knee joint loading compared to walking with a passive backpack. This study provides a framework for future research to further explore the optimization of active backpack assistance for different biomechanical outcomes for those with TTA and other clinical populations with altered gait patterns.

Acknowledgment

The authors would like to thank Eric Hu for his help with the development of the model and optimization framework. This work was supported in part by Award Nos. I01 RX003138 and IK6 RX002974 from the U.S. Department of Veterans Affairs Rehabilitation Research, Development and Translation.

Conflict of Interest

There are no conflicts of interest.

Funding Data

- U.S. Department of Veterans Affairs Rehabilitation Research, Development and Translation (Award Nos. I01 RX003138 and IK6 RX002974).

Data Availability Statement

The datasets generated and supporting the findings of this article are obtainable from the corresponding author upon reasonable request.

References

[1] Sanderson, D. J., and Martin, P. E., 1997, "Lower Extremity Kinematic and Kinetic Adaptations in Unilateral Below-Knee Amputees During Walking," Gait Posture, **6**(2), pp. 126–136.

[2] Neptune, R. R., Kautz, S. A., and Zajac, F. E., 2001, "Contributions of the Individual Ankle Plantar Flexors to Support, Forward Progression and Swing Initiation During Walking," J. Biomech., **34**(11), pp. 1387–1398.

[3] Neptune, R. R., and McGowan, C. P., 2011, "Muscle Contributions to Whole-Body Sagittal Plane Angular Momentum During Walking," J. Biomech., **44**(1), pp. 6–12.

[4] Neptune, R. R., and McGowan, C. P., 2016, "Muscle Contributions to Frontal Plane Angular Momentum During Walking," J. Biomech., **49**(13), pp. 2975–2981.

[5] Zmitrewicz, R. J., Neptune, R. R., and Sasaki, K., 2007, "Mechanical Energetic Contributions From Individual Muscles and Elastic Prosthetic Feet During Symmetric Unilateral Transtibial Amputee Walking: A Theoretical Study," J. Biomech., **40**(8), pp. 1824–1831.

[6] Nasri, A., Abbasi, A., Hadavi, Z., Abbasi, S., and Svoboda, Z., 2024, "Lower-Extremity Inter-Joint Coordination Variability in Active Individuals With Transtibial Amputation and Healthy Males During Gait," Sci. Rep., **14**(1), p. 11668.

[7] Nolan, L., and Lees, A., 2000, "The Functional Demands on the Intact Limb During Walking for Active Transfemoral and Transtibial Amputees," Prosthet. Orthot. Int., **24**(2), pp. 117–125.

[8] Nolan, L., Wit, A., Dudzinski, K., Lees, A., Lake, M., and Wychowanski, M., 2003, "Adjustments in Gait Symmetry With Walking Speed in Trans-Femoral and Trans-Tibial Amputees," Gait Posture, **17**(2), pp. 142–151.

[9] Burke, M. J., Roman, V., and Wright, V., 1978, "Bone and Joint Changes in Lower Limb Amputees," Ann. Rheum. Dis., **37**(3), pp. 252–254.

[10] Silverman, A. K., and Neptune, R. R., 2014, "Three-Dimensional Knee Joint Contact Forces During Walking in Unilateral Transtibial Amputees," J. Biomech., **47**(11), pp. 2556–2562.

[11] Doyle, S. S., Lemaire, E. D., Besemann, M., and Dudek, N. L., 2014, "Changes to Level Ground Transtibial Amputee Gait With a Weighted Backpack," Clin. Biomech., **29**(2), pp. 149–154.

[12] Templin, T. N., Klute, G. K., and Neptune, R. R., 2021, "The Influence of Load Carriage and Foot Stiffness on Knee Joint Loading and Metabolic Cost During Amputee Walking: A Preliminary Modeling Study," J. Prosthet. Orthot., **33**(2), pp. 118–124.

[13] Lefranc, A. S., Klute, G. K., and Neptune, R. R., 2024, "The Influence of Load Carriage and Prosthetic Foot Type on Muscle and Foot Contributions to Support and Propulsion," J. Biomech., **177**, p. 112379.

[14] Ardianuari, S., Morgenroth, D. C., Neptune, R. R., and Klute, G. K., 2025, "Load Carriage Influences Intact Limb Knee Loading Estimate Associated With Osteoarthritis in Individuals With Transtibial Amputation," Clin. Biomech., **124**, p. 106486.

[15] He, L., Xiong, C., Zhang, Q., Chen, W., Fu, C., and Lee, K., 2020, "A Backpack Minimizing the Vertical Acceleration of the Load Improves the Economy of Human Walking," IEEE Trans. Neural Syst. Rehabil. Eng., **28**(9), pp. 1994–2004.

[16] Zhang, Q., Chen, W., Liang, J., Cheng, L., Huang, B., and Xiong, C., 2023, "Influences of Dynamic Load Phase Shifts on the Energetics and Biomechanics of Humans," R. Soc. Open Sci., **10**(8), p. 230636.

[17] Ardianuari, S., Cyr, K. M., Neptune, R. R., and Klute, G. K., 2024, "Should Individuals With Unilateral Transtibial Amputation Carry a Load on Their Intact or Prosthetic Side?," J. Biomech., **177**, p. 112385.

[18] LaPrè, A. K., Price, M. A., Wedge, R. D., Umberger, B. R., and Sup, F. C., 2018, "Approach for Gait Analysis in Persons With Limb Loss Including Residuum and Prosthesis Socket Dynamics," Int. J. Numer. Methods Biomed. Eng., **34**(4), p. e2936.

[19] Hunt, K. H., and Crossley, F. R. E., 1975, "Coefficient of Restitution Interpreted as Damping in Vibroimpact," ASME J. Appl. Mech., **42**(2), pp. 440–445.

[20] Dembia, C. L., Silder, A., Uchida, T. K., Hicks, J. L., and Delp, S. L., 2017, "Simulating Ideal Assistive Devices to Reduce the Metabolic Cost of Walking With Heavy Loads," PLoS One, **12**(7), p. e0180320.

[21] Geijtenbeek, T., 2019, "SCONE: Open Source Software for Predictive Simulation of Biological Motion," J. Open Source Software, **4**(38), p. 1421.

[22] Perry, J., and Burnfield, J., 2010, *Gait Analysis: Normal and Pathological Function*, 2nd ed., CRC Press, Boca Raton, FL.

[23] Winter, D. A., and Yack, H. J., 1987, "EMG Profiles During Normal Human Walking: Stride-to-Stride and Inter-Subject Variability," Electroencephalogr. Clin. Neurophysiol., **67**(5), pp. 402–411.

[24] Geyer, H., and Herr, H., 2010, "A Muscle-Reflex Model That Encodes Principles of Legged Mechanics Produces Human Walking Dynamics and Muscle Activities," IEEE Trans. Neural Syst. Rehabil. Eng., **18**(3), pp. 263–273.

[25] Hansen, N., 2006, "The CMA Evolution Strategy: A Comparing Review," *Towards a New Evolutionary Computation*, J. A. Lozano, P. Larrañaga, I. Inza, and E. Bengoetxea, eds., Springer, Berlin, Heidelberg, Germany, pp. 75–102.

[26] Bhargava, L. J., Pandy, M. G., and Anderson, F. C., 2004, "A Phenomenological Model for Estimating Metabolic Energy Consumption in Muscle Contraction," J. Biomech., **37**(1), pp. 81–88.

[27] Delp, S. L., Anderson, F. C., Arnold, A. S., Loan, P., Habib, A., John, C. T., Guendelman, E., and Thelen, D. G., 2007, "OpenSim: Open-Source Software to Create and Analyze Dynamic Simulations of Movement," IEEE Trans. Biomed. Eng., **54**(11), pp. 1940–1950.

[28] Umberger, B. R., 2010, "Stance and Swing Phase Costs in Human Walking," J. R. Soc. Interface, **7**(50), pp. 1329–1340.

[29] Park, J.-H., Stegall, P., Zhang, H., and Agrawal, S., 2017, "Walking With a Backpack Using Load Distribution and Dynamic Load Compensation Reduces Metabolic Cost," IEEE Trans. Neural Syst. Rehabil. Eng., **25**(9), pp. 1419–1430.

[30] Ventura, J. D., Klute, G. K., and Neptune, R. R., 2011, "The Effects of Prosthetic Ankle Dorsiflexion and Energy Return on Below-Knee Amputee Leg Loading," Clin. Biomech., **26**(3), pp. 298–303.
[31] Koelewijn, A. D., and van den Bogert, A. J., 2016, "Joint Contact Forces Can Be Reduced by Improving Joint Moment Symmetry in Amputee Gait Simulations," Gait Posture, **49**, pp. 219–225.
[32] Grabowski, A. M., and D'Andrea, S., 2013, "Effects of a Powered Ankle-Foot Prosthesis on Kinetic Loading of the Unaffected Leg," J. NeuroEng. Rehabil., **10**(1), p. 49.
[33] Caputo, J. M., and Collins, S. H., 2014, "Prosthetic Ankle Push-Off Work Reduces Metabolic Rate but Not Collision Work in Non-Amputee Walking," Sci. Rep., **4**(1), p. 7213.
[34] Rome, L., Flynn, L., and Yoo, T., 2006, "Biomechanics: Rubber Bands Reduce the Cost of Carrying Loads," Nature, **444**(7122), pp. 1023–1024.
[35] Silverman, A. K., Fey, N. P., Portillo, A., Walden, J. G., Bosker, G., and Neptune, R. R., 2008, "Compensatory Mechanisms in Below-Knee Amputee Gait in Response to Increasing Steady-State Walking Speeds," Gait Posture, **28**(4), pp. 602–609.
[36] Neptune, R. R., Kautz, S. A., and Zajac, F. E., 2004, "Muscle Mechanical Work Requirements During Normal Walking: The Energetic Cost of Raising the Body's Center of Mass Is Significant," J. Biomech., **37**(6), pp. 817–825.
[37] Grumillier, C., Martinet, N., Paysant, J., Andre, J.-M., and Beyaert, C., 2008, "Compensatory Mechanism Involving the Hip Joint of the Intact Limb During Gait in Unilateral Trans-Tibial Amputees," J. Biomech., **41**(14), pp. 2926–2931.
[38] Huang, T. W., and Kuo, A. D., 2013, "Mechanics and Energetics of Load Carriage During Human Walking," J. Exp. Biol., **217**(Pt. 4), pp. 605–613.
[39] Segal, A. D., Zelik, K. E., Klute, G. K., Morgenroth, D. C., Hahn, M. E., Orendurff, M. S., Adamczyk, P. G., Collins, S. H., Kuo, A. D., and Czerniecki, J. M., 2012, "The Effects of a Controlled Energy Storage and Return Prototype Prosthetic Foot on Transtibial Amputee Ambulation," Hum. Mov. Sci., **31**(4), pp. 918–931.
[40] McGowan, C. P., Kram, R., and Neptune, R. R., 2009, "Modulation of Leg Muscle Function in Response to Altered Demand for Support and Propulsion," J. Biomech., **42**(7), pp. 850–856.
[41] Fey, N. P., and Neptune, R. R., 2012, "3D Intersegmental Knee Loading in Below-Knee Amputees Across Walking Speeds," Clin. Biomech., **27**(4), pp. 409–414.
[42] Sharma, L., Hurwitz, D. E., Thonar, E. J., Sum, J. A., Lenz, M. E., Dunlop, D. D., Schnitzer, T. J., Kirwan-Mellis, G., and Andriacchi, T. P., 1998, "Knee Adduction Moment, Serum Hyaluronan Level, and Disease Severity in Osteoarthritis," Arthritis Rheum., **41**(7), pp. 1233–1240.
[43] Lin, X., Yin, S., Du, H., and Leng, Y., 2020, "Improving Energetic Efficiency and Practicality With a Suspended Backpack," IEEE/ASME Trans. Mechatron., **30**(6), pp. 6997–7008.
[44] Bolger, D., Ting, L. H., and Sawers, A., 2014, "Force Asymmetries in Transtibial Amputees for Balance Control," Clin. Biomech., **29**(9), pp. 1039–1047.